agriculture

MDPI

Article

An Intelligent Dual-Axis Solar Tracking System for Remote Weather Monitoring in the Agricultural Field

Tabassum Kanwal [1], Saif Ur Rehman [1,*], Tariq Ali [1], Khalid Mahmood [2], Santos Gracia Villar [3,4,5], Luis Alonso Dzul Lopez [3,4,6] and Imran Ashraf [7,*]

1 University Institute of Information Technology, PMAS Arid Agriculture University, Rawalpindi 43600, Pakistan; tabxmsultan@gmail.com (T.K.); tariq.ali@uaar.edu.pk (T.A.)
2 Institute of Computing and Information Technology, Gomal University, Dera Ismail Khan 29220, Pakistan; khalid@gu.edu.pk
3 Research Group on Food, Nutritional Biochemistry, and Health, Universidad Europea del Atlántico, Isabel Torres 21, 39011 Santander, Spain; santos.gracia@uneatlantico.es (S.G.V.); luis.dzul@unini.edu.mx (L.A.D.L.)
4 Department of Projects, Universidad Internacional Iberoamericana, Campeche 24560, Mexico
5 Department of Projects, Universidade Internacional do Cuanza, Cuito EN250, Angola
6 Department of Projects, Universidad Internacional Iberoamericana, Arecibo, PR 00613, USA
7 Department of Information and Communication Engineering, Yeungnam University, Gyeongsan 38541, Republic of Korea
* Correspondence: saif@uaar.edu.pk (S.U.R.); imranashraf@ynu.ac.kr (I.A.)

Abstract: Agriculture is a critical domain, where technology can have a significant impact on increasing yields, improving crop quality, and reducing environmental impact. The use of renewable energy sources such as solar power in agriculture has gained momentum in recent years due to the potential to reduce the carbon footprint of farming operations. In addition to providing a source of clean energy, solar tracking systems can also be used for remote weather monitoring in the agricultural field. The ability to collect real-time data on weather parameters such as temperature, humidity, and rainfall can help farmers make informed decisions on irrigation, pest control, and other crop management practices. The main idea of this study is to present a system that can improve the efficiency of solar panels to provide constant power to the sensor in the agricultural field and transfer real-time data to the app. This research presents a mechanism to improve the arrangement of a photovoltaic (PV) array with solar power and to produce maximum energy. The proposed system changes its direction in two axes (azimuth and elevation) by detecting the difference between the position of the sun and the panel to track the sun using a light-dependent resistor. A testbed with a hardware experimental setup is designed to test the system's capability to track according to the position of the sun effectively. In the end, real-time data are displayed using the Android app, and the weather data are transferred to the app using a GSM/WiFi module. This research improves the existing system, and results showed that the relative increase in power generation was up to 52%. Using intelligent artificial intelligence techniques with the QoS algorithm, the quality of service produced by the existing system is improved.

Keywords: solar energy; precision agriculture; solar energy tracer; DC motor; light-dependent resistor

Citation: Kanwal, T.; Rehman, S.U.; Ali, T.; Mahmood, K.; Villar, S.G.; Lopez, L.A.D.; Ashraf, I. An Intelligent Dual-Axis Solar Tracking System for Remote Weather Monitoring in the Agricultural Field. *Agriculture* **2023**, *13*, 1600. http://doi.org/10.3390/agriculture13081600

Academic Editors: Francesco Marinello and Maciej Zaborowicz

Received: 30 June 2023
Revised: 9 August 2023
Accepted: 11 August 2023
Published: 13 August 2023

1. Introduction and Background

Agriculture is one of the most important sectors of the economy and plays a crucial role in providing food to the world's population. With the growing demand for food and shrinking fertile land, precision agriculture has become a necessity to improve the yield and quality of crops. One of the key factors that impacts agricultural productivity is weather conditions. Remote weather monitoring systems are increasingly being used to monitor environmental conditions and provide real-time data to farmers to make informed decisions. In this context, the development of a solar tracking system for remote weather

monitoring in agriculture can have a significant impact, improving agricultural productivity while also reducing the dependence on traditional power sources.

In the current age of technology, energy is a crucial topic of discussion, and renewable energy sources such as lunar, thermal, vibration, and wind energies are gaining increasing interest. Since the cost of electricity is increasing every year, renewable energy is considered the best source of energy. However, renewable energy sources are difficult to predict, making it challenging to optimize their production and consumption [1]. A cost-effective energy solution is required to balance supply and demand. Energy storage is becoming increasingly important, and the market for solar energy harvesting is growing rapidly. Ambient energy sources, e.g., solar energy, play an important role in monitoring human activities in the last decade and cannot be underestimated. Over the years, the introduction of energy management schemes that seek to prolong the lifetime of the sensor node and the overall network have been proposed, but the amount of energy required by the sensors to be operational all the time remains a challenge [2,3].

Solar energy has gained tremendous attention in recent years due to various reasons such as the fluctuating price of crude oil, public awareness of environmental issues, supporting policies and subsidies enacted by local governments to boost renewable energy sectors, the price reduction of photovoltaic (PV) panels, etc. Many large-scale solar farms have been commissioned in the US, Europe, and China, as the global PV price has been dropping rapidly in recent years, which is in agreement with Swanson's law [4]. However, PV-generated electricity is not competitive enough compared to fossil fuels (oil, gas, and coal), especially in urban areas. Hence, more extensive research and development on PV cell material science is required to overcome the conversion efficiency hurdle and reduce manufacturing costs. Meanwhile, several approaches other than exploring new materials for PV cells have been proposed. For instance, a concentrated photovoltaic (CPV) system was designed to concentrate large amounts of sunlight into PV cells [4,5]. Similarly, a maximum power point tracker can draw maximum power by tracking and operating on the maximum power point of the PV arrays [6], and solar tracking can enable a maximized power captured from the sun by following the sun path [7]. These methods can increase the energy production of PV to various degrees of success. Above all, solar tracking poses a great advantage to enhance the PV system efficiency as compared to a static solar system [8]. A dual-axis solar tracker (DAS) is a type of solar tracker with two rotational axes, which always enable it to align the PV panels and point directly towards the solar disk [9,10]. Solar irradiance (W/m^2) is a measure of the amount of sunlight that falls on a surface. It is the most fundamental factor in determining the performance of a PV panel to be underestimated. Over the years, the introduction of energy management schemes has led to many efficient approaches [11].

A single-axis system may require more space to accommodate the solar panels and collects energy along one axis, which reduces its efficiency. A dual-axis solar tracking system is designed to follow the sun and optimize the amount of sunlight collected by PV cells. The system follows the sun's movement in both the horizontal and vertical planes, from east to west and north to south, respectively. It is widely used in the agricultural field to optimize the amount of collected solar energy, thereby increasing the efficiency of the system. Wireless sensor networks (WSNs) are making a huge impact among emerging technologies [12]. WSNs have consistently ranked highly in this field of research for over a decade [13]. Since the system is WSN-based, the term quality of service (QoS) is defined as the network's assurance to fulfill the desired services for an individual, including delay and other parameters. To meet the QoS requirements, the optimal path between the source and destination needs to be located, and other components for QoS are resources, request, response, and reservation [14]. The authors [15] conducted a study that explored the primary parameters of QoS which include delay, loss, jitter, and latency. However, extending QoS to WSNs faces several challenges due to features such as mobility, radio channel frequency, and battery issues [9]. Numerous research institutes have worked in this field and developed research projects that have made significant advancements in all

aspects, including hardware, software, design, and standard applications [16]. WSNs are special-purpose equipment that gather information from the physical world and transmit it to users and applications, such as environmental monitoring, military operations, agriculture, and energy efficiency [17].

As energy is crucial to power various operations and applications, relying solely on electricity is not always a cost-effective solution. Renewable energy production, on the other hand, provides a better alternative for such requirements [18]. One type of energy collection system is the solar harvesting system, which converts heat into energy [19]. Intensive research has led to the optimization of QoS for solar systems. The main aim is to explore new developments and interests in this field [20]. Energy collection systems are used to gather strength from background resources. The energy harvesting system produces power that can be utilized for various applications [21]. The equation for converting heat into electrical energy in a solar harvesting system [22] is

$$P = \eta AG * FF \tag{1}$$

where P is the electrical power output, η is the conversion efficiency, A is the solar panel area, G is the solar irradiance, and FF is the fill factor of the solar cells. The formula for calculating Quality of Service (QoS) in a Wireless Sensor Network (WSN) [17] is

$$QoS = (1 - \alpha) * R + \alpha * C \tag{2}$$

where R is the reliability, C is the coverage, and α is the weight given to each parameter. The formula for calculating delay in a WSN [13] is

$$Delay = T_{end} - T_{start} - t_{proc} - t_{queue} - t_{trans} - t_{prop} \tag{3}$$

where T_{end} is the time when the packet is received, T_{start} is the time when the packet is sent, t_{proc} is the processing time, t_{queue} is the queuing delay, t_{trans} is the transmission delay, and t_{prop} is the propagation delay. The equation for estimating solar irradiance on a tilted surface [18] is

$$G = G_b * cos(\theta) + G_d * \frac{(1 + cos(\theta))}{2} + G_r * \frac{(1 + cost(\theta))}{2} \tag{4}$$

where G_b is the beam irradiance, G_d is the diffuse irradiance, G_r is the reflected irradiance, and θ is the angle of incidence of the sun on the tilted surface.

Solar-based energy tracking systems are proving to be fruitful for various industries, providing more output than other types of systems. It is expected that solar tracking systems will be the best systems for energy sources in the future, with their output efficiency depending on the tracking method used and weather conditions [23]. Energy harvesting technologies are the best option to fulfill the needs of different fields [24]. Energy harvesting is defined as a technique that is used to capture, harvest, and gather unused resources of natural energy such as energy produced from the sun, wind, ocean, etc. These natural resources are big energy sources and can provide large-scale harvested energy [25]. The energy harvesting system consists of four main parts, namely, harvester, energy collector, power manager or conditioning circuit, and energy storage unit [26]. As a result, several energy harvesting, energy optimization, and distribution approaches have been designed recently.

In [27], the authors developed a particle swarm optimization (PSO), which is modeled after the social behavior of animals such as fish schooling and birds flocking. This approach employs a swarm of artificial agents or particles, and each agent's motion is influenced by three factors. It involves separation, where agents maintain a safe distance; alignment, where each agent moves toward the average behavior of the swarm; and cohesion, where each agent moves toward the average behavior of its neighbors. Several unused ambient energy resources are available that can be utilized for energy harvesting. These energy

resources are enough to meet our energy needs and there is no need for extra resources such as burning fossil fuels to rotate turbines to produce energy [28]. Environmental resources are renewable and can exist for a longer period. Different experiments have been performed to find energy resources that could be produced from natural resources [29].

The study [30] increased the overall efficiency of the energy harvesting system in WSN using maximum power point tracking (MPPT) techniques coupled with an artificial intelligence (AI)-based algorithm. Simulations for the system were run using Matlab 2021b. After a successful simulation, a testbed was built to verify the results. An AI neural network algorithm was deployed to obtain solutions to problems that are hard to solve using common methods such as pattern matching, computer vision, design identification, speech credit, classification, and control system. Neural network models are similar to learning algorithms, but may vary in terms of rules, parameters, weights, and network structures [31].

The study [32] designed an energy management scheme using a trio energy management scheme for harvesting, transferring, and conserving energy. This maintained the network lifetime to make it more operation and efficient. However, the cost of experimentation, testbed installation, and simulation tools were expensive. Similarly, [33] presented an MPPT-based energy harvesting scheme using a perturbation-based micro-solar approach. Results indicated increased efficiency with lower overhead.

The authors presented an ambient-energy-based solution for WSN networks in [34]. The authors employed a pulse width modulation scheme and MPPT approach to increase the efficiency of the system by 87%. The study [35] created a method for selecting optimal parameters of the PSO by considering the topology and parameters of the DC–DC converter and other configuration settings of solar panels. The parameters of a buck converter connected to a battery were estimated using the newly proposed approach. The authors used weaseled, distributed cluster head re-selection and polynomial time-scheduling algorithms for that purpose. The outcomes indicated that improved performance can be obtained with reduced battery depletion. To address these challenges, we present the proposed model outlined in the following section. Table 1 provides an overview of existing works in this field.

In this paper, we have provided a solar energy harvesting scheme that, when fully implemented, reduces the issues of limited energy. The main source of solar power is the sun, which can be used to obtain solar energy. The sun's rays strike the earth, delivering 174,000 terawatts of energy, which can be used for our needs. This alone makes the solar panel the best choice for a renewable energy source—according to the United Nations Development Program in 2000, if we can harness the full power of the sun's rays coming to Earth, we can create 1575 to 49,837 Joules of energy, which is far greater than the world's needs. However, the problem lies in the solar panel, i.e., that the technology behind the solar panel is not efficient enough to fully harness this abundant energy. Thus, to make the soar panel more efficient, we created a movable solar panel that can adjust its position regarding the sun's current position to obtain the optimal sunlight. In addition to energy maximization, the proposed system can also give parameters such as humidity, temperature, and air quality from the remote agricultural fields onto the mobile app, which can greatly facilitate the farmers to make informed decisions. The main contributions of this research study are as follows:

- To improve the efficiency of solar panels, the paper proposes a solar tracking system with dual axes that can move to adjust its position. The solar tracking system aims to maximize energy generation by optimizing the orientation of the solar panels;
- The proposed system not only maximizes energy but also provides additional parameters such as humidity, temperature, and air quality from remote agricultural fields;
- The collected parameters can be accessed through a mobile app, making it easier fo farmers to monitor and manage their agricultural activities. The implementation of the proposed system shows enhanced energy generation and provides valuable data for agricultural purposes.

The article is structured as follows. Section 2 presents the proposed approach. Results are discussed in Section 3. At the end, Section 4 provides the conclusion.

Table 1. Comparative analysis of various state-of-the-art approaches.

Ref.	Findings	Framework	Results	Limitations
[32]	Provided the energy management scheme	Trio energy management scheme: energy harvest, transfer, and conservation	Maintaining the network lifetime. Balance the energy. Network more operational and efficient	Cost of experimentation using testbeds. Simulation tools were not supportive of energy
[33]	Proposed harvesting: MPPT, energy storage, and cold booting. Examined technical issues with solar energy harvesting. Compared batteries and supercapacitors	Perturbation-based MPPT micro-solar MPPT approach or load-matching sensor-driven MPPT	Increased efficiency, achieving low overhead, achieving a balance between high and low output	Implementation issues. Storage issues
[34]	Solution to the problem of WSN nodes by ambient solar energy	Solar energy harvesting system. Pulse width modulation (PWM) and maximum power point tracking (MPPT)	Increased efficiency 87%, PWM efficiency, and 96% efficiency by MPPT	Advanced MPPT algorithms such as NN, Fuzzy logic not used
[35]	Hybrid cluster-heads framework	Weaseled, distributed cluster-head re-selection and a polynomial time-scheduling algorithm	Reduced battery depletion by 20%, overcame cost by 25%, improved network performance.	Performance increased but system cost was compromised
[36]	Presented a model of a bi-stable energy harvester	Bi-stable energy harvester improved performance	Generated a larger power output	Non-guaranteed QoS
[37]	Gave power control policy	QoS-driven power control policy joined energy, harvesting Water Filling (E-WF) scheme, harvesting Channel	Optimized the Effective Energy Policy (EEE)	Guaranteed QoS but cost factor compromised
[38]	Proposed algorithm to optimize the sensor's operational ability	Design of an energy harvesting system, solar energy prediction model, downgrade function algorithm	Improved the QoS. Resolved optimization problems on low-power sensors	No guarantee of the solutions, high-cost computational algorithms cannot be embedded into resource-constrained sensors

2. Materials and Methods

2.1. Proposed Model

The block diagram of the proposed system is illustrated in Figure 1. The diagram illustrates that the values from the LDRs are sent to the Arduino's microcontroller (Arduino, Somerville, MA, USA),then the difference between the values is calculated. Based on the results, the relevant motor then moves to make the PV perpendicular to the sun and this process will repeat itself throughout the day. Here, sun position can be calculated from the sun position algorithm and panel position can be calculated from angle sensors connected to the tracker. Here, the sun position and PV panel position are both given as inputs to the microcontroller, which rotates the panel to an exact position through the DC motor with the help of the motor driver and relay. For measuring temperature and humidity, we used the DHT11 sensor (AOSONG Electronics, Guangzhou, China) and, for air quality, we used the MQ135 sensor (Winsen Sensor, Zhengzhou, China. The sensors measure the value and send it to the WiFi module; the WiFi module then sends the value to the real-time database, which is then shown on the app with their graphical representation.

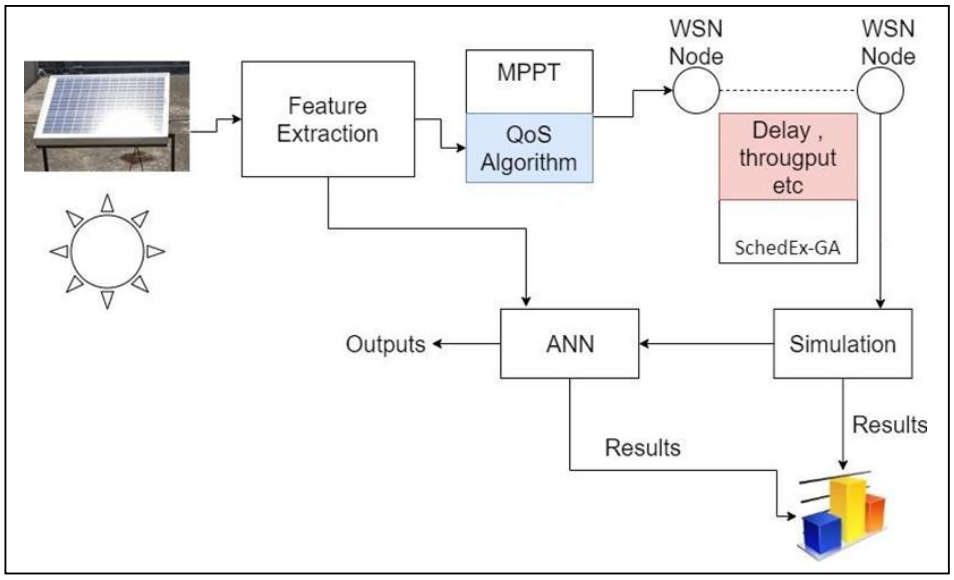

Figure 1. Block diagram of the proposed model.

The testbed was developed to test the solar tracker and functionality of weather monitor sensors such as the temperature sensor and gas sensor, as shown in Figure 2. We used DHT11 as the temperature and humidity sensor and MQ135 as the gas sensor, which was used to measure CO_2 in the air. The solar tracker used LDRs to measure sun luminosity and give a value based on it. The values were then collected and averages were taken to decide in which direction the solar panel would rotate. The power produced by it was then used to power the sensor, whose value could be seen on the laptop on an Arduino serial monitor and sent to the cloud for further monitoring and use. Specifications of the testbed are shown in Table 2.

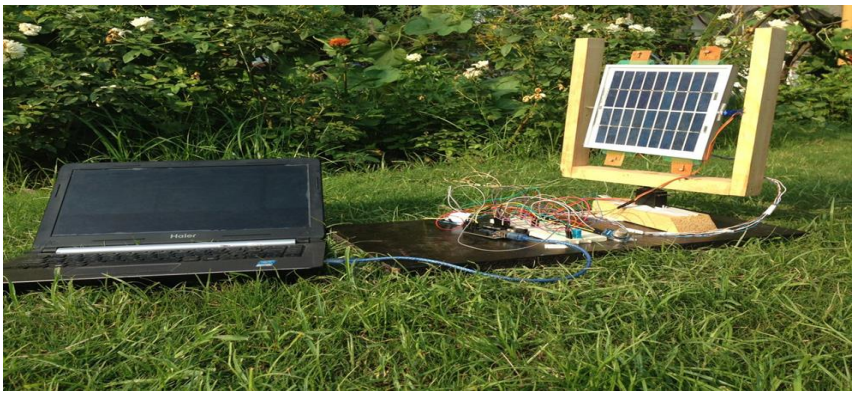

Figure 2. Experimental setup.

Table 2. Testbed specifications.

Component	Specifications	Average Value
Solar Panel	Type: Photovoltaic	-
	Capacity: [Watts or Kilowatts]	300 W
	Dimensions: [Length × Width × Thickness]	1650 mm × 992 mm × 40 mm
	Material: [Monocrystalline, Polycrystalline, etc.]	Monocrystalline Silicon
	Operating Voltage: [Volts]	36 V
	Temperature Coefficient: [%/°C]	−0.3% per °C

Table 2. *Cont.*

Component	Specifications	Average Value
Controller	Type: Intelligent dual-axis solar tracking	-
	Tracking Algorithm: [Description]	Sun Tracking Algorithm
	Power Supply: [Input Voltage and Power]	24 V DC, 10 W
	Tracking Accuracy: [Degrees or Percentage]	$\pm 0.5^{\circ}$
	Control Modes: [Manual, Automatic]	Automatic
Power Converter	Type: Bidirectional	-
	Maximum Power Point Tracking (MPPT): [Yes/No]	Yes
	Input Voltage Range: [Volts]	150–600 V
	Output Voltage: [Volts]	230 V
Sensors	Weather Sensors: [List of Weather Sensors]	Temperature, Humidity DHT11
	Power Supply: [Battery-operated, Solar-powered]	Solar-powered

The system was comprised of several sensors which are briefly described here.

2.1.1. DHT11 Sensor

The DHT11 is a basic digital temperature and humidity sensor. It provides a digital output representing temperature and humidity values. The power requirements for the DHT11 sensor are as follows:

Operating Voltage: 3.3 V to 5 V (typically powered with 5 V for most applications);
Operating Current: Around 2.5 mA to 3 mA during data acquisition;
Standby Current: Minimal standby power consumption.

It is important to note that the DHT11 does not have advanced power-saving features, and it draws a consistent current during data acquisition. When using the sensor in battery-powered projects, it is advisable to keep the power consumption in mind to optimize battery life.

2.1.2. MQ135 Sensor

The MQ135 is a gas sensor primarily used to measure air quality and detect various harmful gases like NH_3, NO_x, alcohol, benzene, smoke, and CO_2. The power requirements for the MQ135 sensor are as follows:

Operating Voltage: 5 V (typically powered with 5 V for most applications);
Heater Power: The MQ135 sensor requires a preheat time to stabilize readings. It has an internal heater element that consumes around 120 mA to 150 mA during the preheating phase;
Operating Current: After preheating, the operating current drops to around 40 mA during gas sensing;
Standby Current: Minimal standby power consumption after preheating.

The daily electrical load schedule is given in Table 3, while yearly analysis on the solar panel is carried out in the following sections.

Table 3. Daily electrical load schedule.

Time	Power Source	Activity
8 am to 6 pm	Solar Panels	Measuring system powered by solar energy. Excess energy charges the battery.
6 pm to 8 am (next day)	Battery	Measuring system operates on stored energy from the battery.

2.1.3. Sensor and Actuator Accuracy and Ranges

DHT11 Temperature Sensor:
Accuracy: ±2 °C;
Measurement range: 0 °C to 50 °C.
DHT11 Humidity Sensor:
Accuracy: ±5%;
Measurement range: 20% to 90% RH.
MQ135 Air Quality Sensor:
Accuracy: ±10%;
Measurement range: 0 to 1000 ppm CO_2.
LDR Light Sensors:
Accuracy: ±10%;
Measurement range: 0 to 1000 lux.
DC Motors:
Position accuracy: ±1%;
Speed control accuracy: ±5%.

2.2. Proposed Artificial Neural Network

A neural network model is very efficient to solve complex problems. In this research, an artificial neural network (ANN) was deployed to resolve the problem of optimizing the quality of the harvesting system, in which we needed to determine the existing pattern and compare it with new results. The gaps in existing results could be found using the backpropagation neural network technique. ANN is composed of interconnected elements called neurons, which compute values from input and give the necessary output to solve complex problems. In this project, the ANN model is deployed to investigate the energy harvesting system for the alternative prediction in comparison to the input function to obtain better efficiency and optimization.

Backpropagation was used for the training of ANN, in which neurons were trained according to a given pattern. Proper training of neurons ensures the lowest error rate. Backpropagation is a learning algorithm that is mainly used by a multilayer perceptron. In this type of technique, results or outputs are compared with given values. The learning procedure adjusts the links between layers to optimize output. The main reason to select this method was its ability to perform a specific task or solve problems, i.e., it is required to train a model with certain data. The network was trained based on specific values, which improved with time using the backpropagation algorithm. At the start, weight distributions were random, and prediction was also random. Then, after a specific interval of time, the optimization step was completed by comparing the output with the output values which were already known.

2.3. Power of the Measuring System

The power consumption of a measuring system depends on several factors, including the number of sensors, data transmission frequency, data processing components, and power management efficiency. A brief overview is provided in Table 4.

Table 4. Components and their corresponding power consumption.

Component	Power Consumption (Approx.)
Sensors (Temperature, Humidity)	5 to 10 Watts
Data Logger and Communication Module	5 to 10 Watts
Power Supply (Solar Panel Array + Battery)	50-Watt solar panel array + 100 Ah battery capacity

2.4. Algorithm for QoS Optimization

The sun position algorithm was used to determine the position of the sun at a given time for a specific location, using Algorithm 1. The position of the sun relative to the earth is affected by the revolution and rotation of the earth. Therefore, the sun's position depends on the time, date, and geographic location: longitude (0 to 180°) and latitude (0 to ±90°). The position of the sun was calculated by universal time. World time and daily time were based on universal time. The metric T was the difference between two-time scales:

$$\Delta T = TD - UT \tag{5}$$

Algorithm 1 Algorithm for QoS optimization

Input Parameters: Local date, Time, Time Zone, Location (latitude and longitude), Altitude

1: Conversion of UTC time into TDT
2: Calculate the angle of declination
$D = arc\ sin(sin(22.439 - 0.00000036 * (JD - 2451545)) * sin(L))$
3: Calculate sun transit
$Transit = 12 + TZ - (\frac{L}{15} - EqT)$
The time equation can be used as
$EqT = \frac{q}{15} - RA$
where RA is
$RA = arc\ tan(cos(22439 - 0.00000036 * (Id - 2451545)) * \frac{Sin(L)}{Cos(L)}))$
4: Conversion of transit time from UTC to TDT
5: Using the declination angle of the sun and transit time, sunrise and sunset times can be obtained

3. Results

To evaluate the performance of our model and algorithm, we conducted various experiments. The results of these experiments are presented in the following sections.

3.1. System Efficiency

We must compare the power provided by the sun to the electricity generated in order to determine the efficiency of the panel. A panel would be 100% efficient if it could convert all of the light that struck it into energy. Unfortunately, achieving such efficiency is impossible. We used the following equation to analyze the efficiency of the proposed system (the length and width of the panel are given in meters (m)):

$$Efficiency = \frac{Panel\ power\ (kW)}{Panel\ length \times Panel\ width \times Solar\ irradiance} \times 100 \tag{6}$$

3.2. Daily Analysis

Different experiments were carried out in the spring season to evaluate the performance of the proposed approach. Table 5 shows the average values of different experiments. These values then can be used by the farmers for making further decisions. These real-time data on weather parameters such as temperature, humidity, etc. can help farmers make informed decisions on irrigation, pest control, and other crop management practices.

Table 5. Average value of different experiments.

	Temperature	Humidity	Air Quality
Experiment 1	29 °C	59%	1464 ppm
Experiment 2	29 °C	60%	1346 ppm
Experiment 3	29 °C	60%	1314 ppm
Experiment 4	29 °C	60%	1367 ppm

Table 5 shows the average values across multiple test days, rather than being tied to a specific date. The metrics such as temperature, humidity, and air quality were averaged across several experiments. Even without the specific dates, these data can still provide some useful insights:

- The temperature range and fluctuations give an indication of typical conditions that may be experienced. This could help with system design considerations;
- The humidity and air quality averages establish baseline levels for the location. This is valuable reference information;
- The diurnal temperature profile shows the temperature variation over a 24 h cycle. This can inform solar energy generation modeling;
- The values then can be used by the farmers for making further decisions. These real-time data on weather parameters such as temperature, humidity, etc. can help farmers make informed decisions on irrigation, pest control, and other crop management practices.

Figure 3 provides a graph representing temperature values obtained from a temperature sensor installed on the system. The temperature data were recorded at regular intervals, typically hourly. These recorded values can be utilized by farmers for various purposes. Upon observing the graph, it becomes apparent that the temperature fluctuates within specific ranges throughout the day. By glancing at the graph, one can easily identify the highest and lowest temperature points.

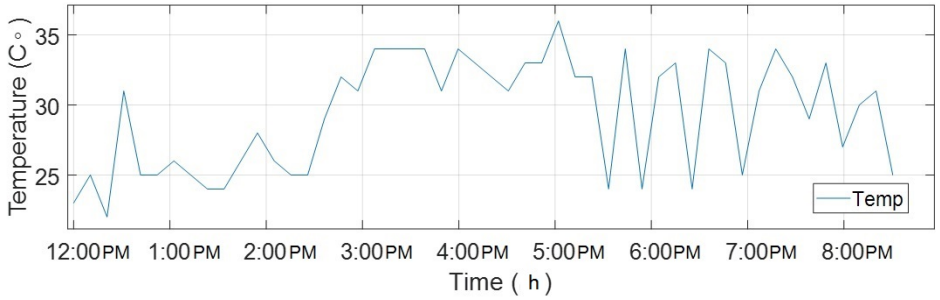

Figure 3. Day 1 temperature analysis graph.

On day 1, as shown in Figure 4, the humidity demonstrated a rising trend as the day progressed. This indicates that the humidity levels increase gradually over time. Simultaneously, the carbon dioxide levels showed a decreasing trend, suggesting a decline in the concentration of carbon dioxide in the environment. Thus, the graph illustrates the trend of humidity increasing as the day progresses, while the levels of carbon dioxide decrease. The temperature readings generally remained within a favorable range. However, there was a spike in temperature at some point, which can be attributed to irregularities in the sensors used for measurement.

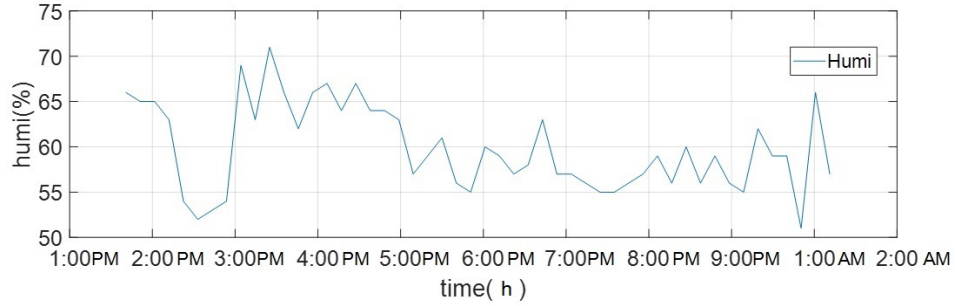

Figure 4. Day 1 humidity analysis graph.

In the results for experiment 2, shown in Figure 5, a similar trend is observed, with the graphs displaying small variations in values. The temperature readings ranged between 25

and 35 degrees, indicating a relatively stable temperature range. The temperature graph shows that the temperature remained within a favorable range of 25 to 30 degrees Celsius throughout the day. This consistent temperature level suggests stable conditions. However, it is important to note that there was a spike in temperature at some point, which can be attributed to irregularities or inaccuracies in the sensors used to measure temperature. Overall, the observed trends on day 1 indicate increasing humidity, decreasing carbon dioxide levels, and a stable temperature within a desirable range. The irregular temperature spike should be considered with caution due to potential sensor inaccuracies.

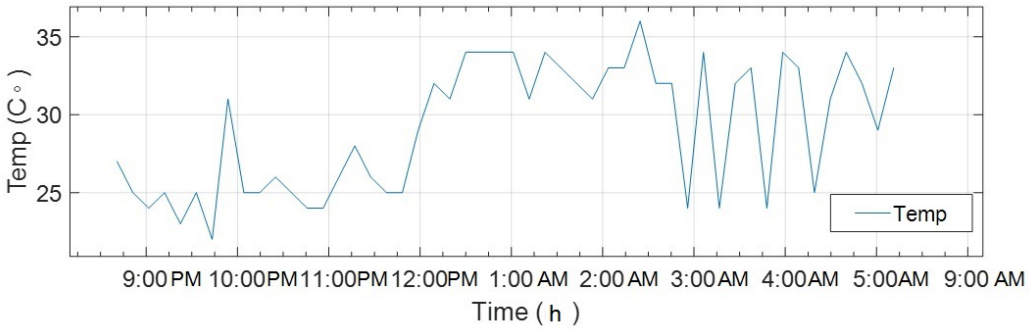

Figure 5. Day 2 temperature analysis graph.

Figure 6 shows that the humidity values fluctuated within a narrow range of 55 to 57 points. This suggests a consistent level of humidity throughout the experiment. The close proximity of the temperature and humidity values implies a potential correlation between these two variables. The similarity in trends between experiment 1 and experiment 2 may indicate that the factors influencing temperature and humidity remain relatively constant or have similar patterns during both experiments. It is worth noting that further analysis and data collection would be necessary to determine the significance and implications of these observations accurately.

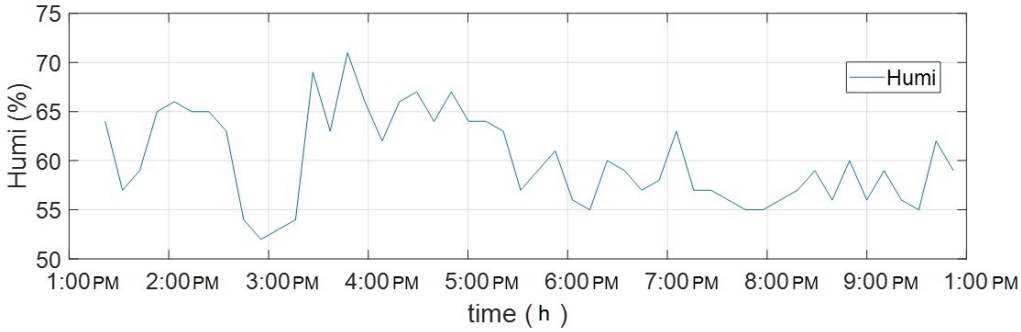

Figure 6. Day 2 humidity analysis graph.

On day 3, as shown in Figure 7, a similar trend to the previous days was observed. The temperature graph indicates that the temperature ranged between 23 and 26 degrees Celsius, with small variations within this range. Similarly, the humidity values fluctuated between 51 and 65 points, suggesting relatively stable humidity levels. The consistency in the trends of temperature and humidity between day 1, day 2, and day 3 may indicate a continued pattern or stable environmental conditions during this period.

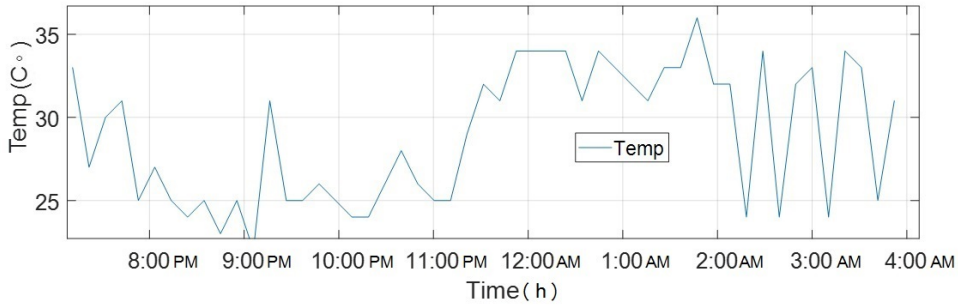

Figure 7. Day 3 temperature analysis graph.

On day 3 as shown in Figure 8, the humidity demonstrated a rising trend as the day progressed. This indicates that the humidity levels increase gradually over time. Simultaneously, the carbon dioxide levels showed a decreasing trend, suggesting a decline in the concentration of carbon dioxide in the environment.

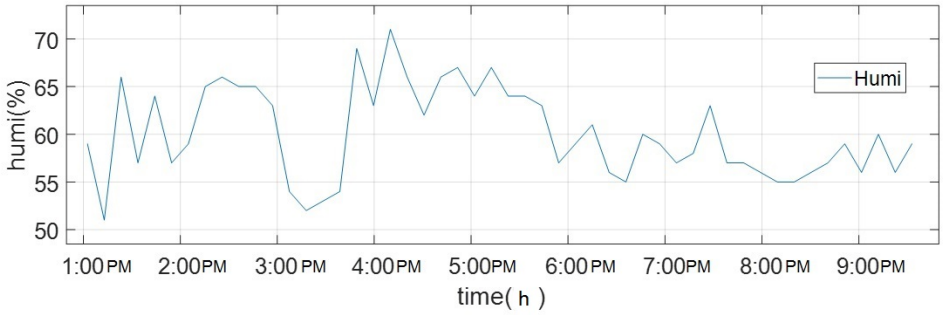

Figure 8. Day 3 humidity analysis graph.

In experiment 4, as shown in Figure 9, a distinct trend was observed, where the temperature increased as the day progressed, indicating hotter days. The temperature readings staredt at 20 degrees and gradually rose to 35 degrees. This trend aligns with scientific understanding, as temperatures tend to increase during the daytime due to factors such as solar radiation and atmospheric conditions. Additionally, it is noted that the nights were colder, suggesting a drop in temperature during nighttime hours. This is a common occurrence, as heat is radiated back into the atmosphere during the night, resulting in cooler temperatures. Furthermore, the maximum temperature recorded during the day reaches a high, indicating a particularly hot day during the course of the experiment.

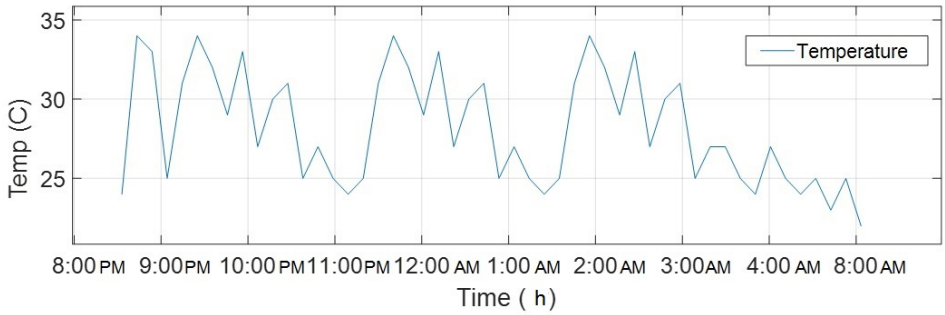

Figure 9. Day 4 temperature analysis graph.

The provided graphs, as shown in Figure 10, represent humidity values and air quality values obtained from a temperature sensor placed in a system. The humidity values were recorded per minute, while the air quality values specifically measured carbon dioxide (CO_2) levels and were also recorded per minute. These values were collected at regular intervals and can be utilized by farmers for various purposes. In the humidity graph, it

can be observed that there were fluctuations in humidity levels. Notably, when water was sprinkled or introduced into the system, the humidity level varied accordingly. This suggests that the addition of water affects the humidity levels, which can be valuable information for farmers in determining irrigation or moisture management strategies.

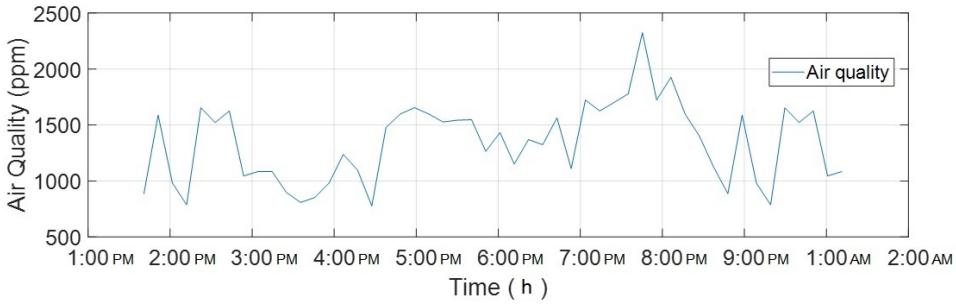

Figure 10. Day 1 air quality analysis graph.

In the air quality graph, the values represent the concentration of carbon dioxide in the air. It is evident that the CO_2 levels varied over time, and there were distinct increases in value when plants released carbon dioxide. This information can be beneficial for farmers to monitor the health and growth of plants and potentially adjust ventilation or other environmental factors to optimize plant growth. The availability of real-time humidity and air quality data can assist farmers in making informed decisions regarding irrigation, moisture control, and environmental management practices, ultimately improving agricultural productivity and plant health.

In the air quality graph, as shown in Figure 11, the values represent the concentration of carbon dioxide in the air. It is evident that the CO_2 levels varied over time, and there were distinct increases in value when plants released carbon dioxide. This information can be beneficial for farmers to monitor the health and growth of plants and potentially adjust ventilation or other environmental factors to optimize plant growth.

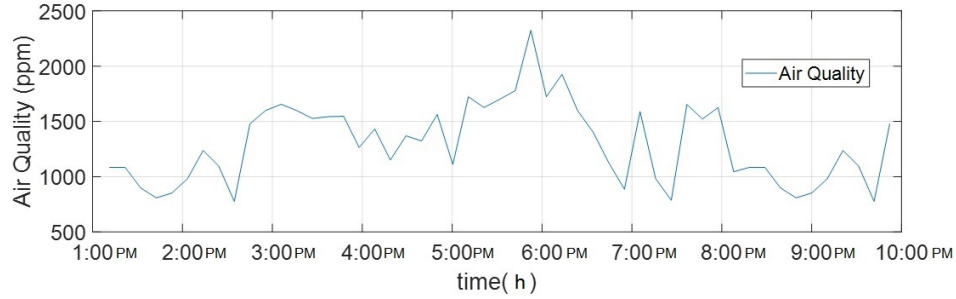

Figure 11. Day 2 air quality analysis graph.

3.3. Annual Analysis

Based on the results obtained from various systems observed over the course of a year, it has been found that the dual-axis system exhibited the highest output efficiency, specifically measuring 98.7%. In comparison, the horizontal-axis system achieved an output efficiency of 98.2%, while the vertical-axis system achieved an output efficiency of 98.3%, both with a sloped angle. These output efficiency values indicate the effectiveness of each system in converting irradiance (solar energy) into usable output. The higher the output efficiency, the more effectively the system is able to harness solar energy and convert it into usable forms such as electricity or heat. To further understand the context and implications of these findings, the irradiance values are provided. Irradiance refers to the power per unit area received from the sun, typically measured in Watts per square meter. Figure 12 presents the likely variations in irradiance throughout the year, which can help explain the differences in output efficiency observed across the different systems. By

analyzing the irradiance values and correlating them with the system's output efficiency, it becomes possible to gain insights into how solar energy availability and intensity impact the performance of each system.

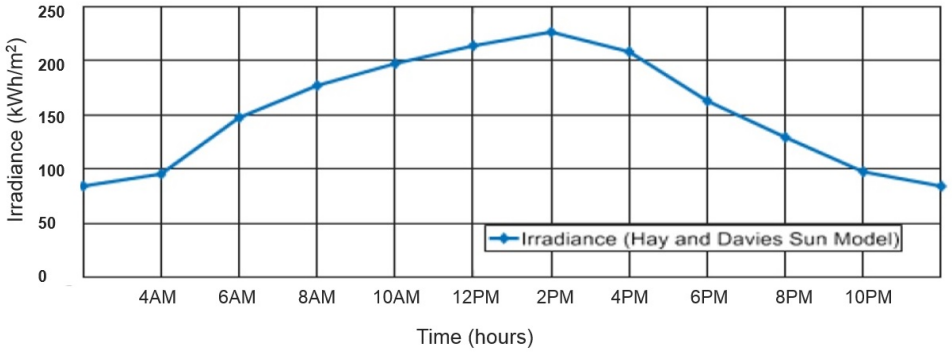

Figure 12. Irradiance values.

In Figure 12, the graph displays the values of irradiance generated from a simulation over a one-year time period. The graph likely shows the variations in irradiance levels throughout different seasons or months of the year. The purpose of this comparison is to evaluate the performance of a simple harvesting system that lacks a tracking feature. It is observed that the simple system, without tracking, is unable to capture the full irradiance available. As a result, the system experiences lower output power compared to the simulated values of irradiance. The comparison of the difference in performance of different components is provided in Table 6.

Table 6. Production efficiency of different components.

Solar Panel System	Description	Yearly Energy Efficiency (Approx.)
Dual-Axis Tracking	Dual-axis solar panels can track the sun both horizontally and vertically	98.7%
Single-Axis Tracking	Single-axis solar panels can only track the sun along one axis (usually east–west)	98.2%
Fixed Tilt	Fixed-tilt solar panels remain stationary and do not track the sun's movement	98.3%

The comparison between the simulated irradiance values and the performance of the simple system highlights the importance of tracking features in maximizing the capture of solar energy. Tracking systems are designed to align solar panels or collectors with the direction of the sun, optimizing the absorption of sunlight and increasing output efficiency. The lower output power of the simple system underscores the potential benefits of implementing more advanced tracking systems, such as dual-axis or other sophisticated tracking mechanisms. These systems can adjust their position to follow the sun's path, ensuring optimal exposure to irradiance and maximizing the energy harvested from solar sources. This comparison serves as evidence supporting the use of tracking systems for enhancing the performance and output power of solar harvesting systems. In the provided figure, it is documented that the dual-axis tracking system has demonstrated the capability to capture the highest amount of sunlight or sun rays throughout the year. The graph likely depicts the irradiance values or solar energy received by the dual-axis tracking system over different time periods.

Furthermore, a comparison was made between the horizontal system and the dual-axis tracking system, as shown in Figure 13. It is observed that the horizontal system, which is a fixed system without any tracking capability, exhibits a consistent and linear line over the entire year on the graph. This implies that the horizontal system does not adjust

its position to track the movement of the sun. In contrast, the dual-axis tracking system, which has the ability to adjust its position both horizontally and vertically to track the sun's movement, shows more variability in irradiance values over the year. This indicates that the dual-axis tracking system is able to align itself optimally with the sun's position, maximizing the capture of sunlight and resulting in higher irradiance levels compared to the fixed horizontal system.

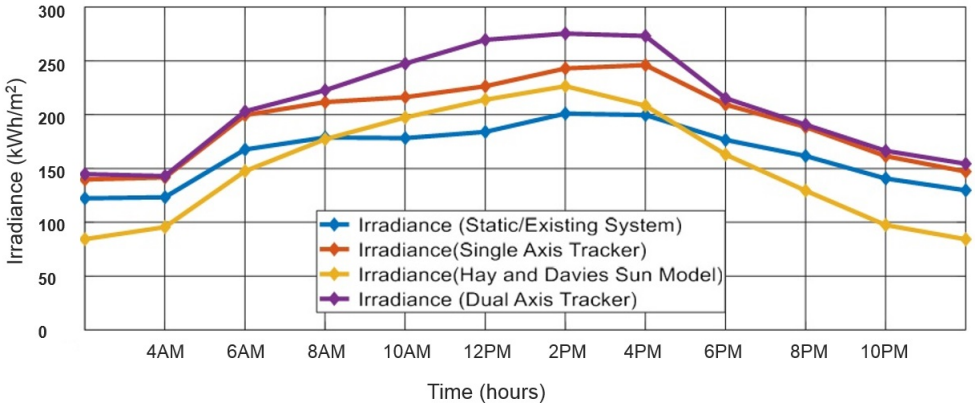

Figure 13. Irradiance values.

The comparison between the two systems further emphasizes the advantages of incorporating tracking capabilities in solar harvesting systems. By tracking the sun's movement throughout the day and year, the dual-axis system can consistently optimize its orientation and capture a higher amount of sunlight, leading to increased irradiance and potentially higher energy output. These findings highlight the importance of considering tracking systems, such as the dual-axis system, for maximizing solar energy utilization and enhancing the performance of solar harvesting systems.

3.4. Performance of Artificial Neural Network

The best validation performance is described with the help of Figure 14, in which the system's performance is explained after running an ANN simulation. Results obtained after simulation showed that performance remains stable at the same value but, without using this, it may decrease over time. In Figure 14, the histogram shows that there were many faults but, after using the ANN technique, quality increased.

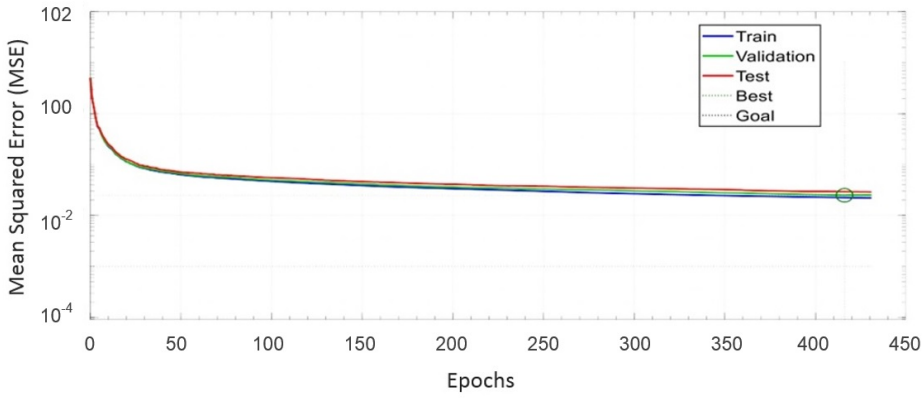

Figure 14. Validation performance of ANN. The best validation performance is 0.024918 at epoch 416.

A neural network was proposed to optimize the system's efficiency. It contained different layers—3, 10, and 15 layers and neurons were used to obtain an optimal architecture. The data were split into train, test, and validation sets. The training process proceeded, provided that the system continuously enhanced the authentication established. The test pair offered an autonomous way of measuring network precision completely.

The final architecture of ANN contained 3 hidden layers, each with 10 neurons, while the output had 3 possibilities. This structure provided the best functionality in classification among all examined architectures. The number of epochs used for training the ANN was 500; however, the best results were obtained at 416 epochs. A histogram analysis of ANN is shown in Figure 15. For training ANN, there were three algorithms:

- Levenberg–Marquardt;
- Bayesian Regularization;
- Scaled Conjugate Gradient.

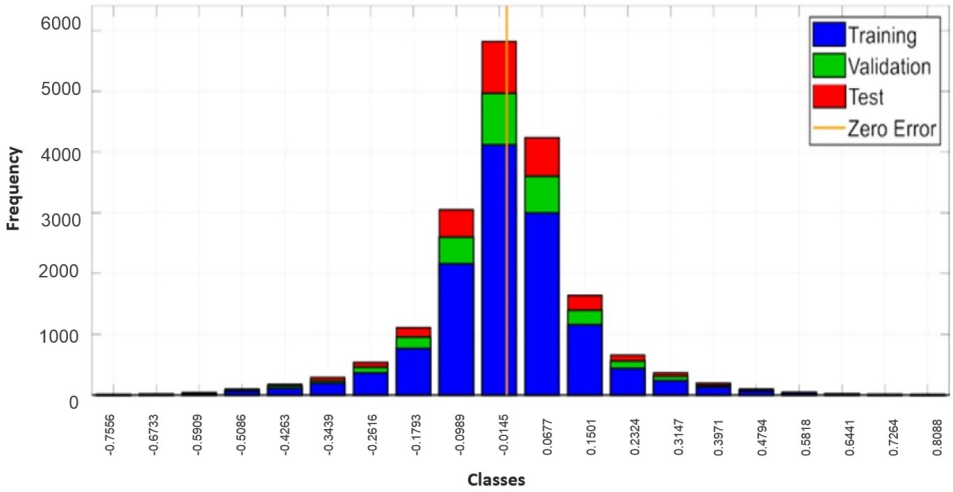

Figure 15. Error histogram for ANN.

The Levenberg–Marquardt algorithm consumes more memory, but, positively, it takes less time. Training automatically halts when there is no further improvement in generalization. This algorithm was chosen for simulation. In the Bayesian regularization procedure, more time is consumed but the output is satisfactory, even for datasets which are small, noisy, or difficult. The process stops with weight minimization. A scaled conjugate gradient algorithm does not use more memory. It stops when there is no further improvement, which is identified by increasing the value of the mean square fault of a sample.

3.5. Important Characteristics of the Proposed Approach

The approach presented in this paper improves the existing system in several ways:

- **Improved Efficiency:** The main objective of this research is to enhance the efficiency of solar panels in providing constant power to sensors in agricultural fields. By implementing a solar tracking system that changes its direction in two axes based on the sun's position, the proposed approach optimizes the orientation of the solar panels for maximum energy generation;
- **Real-time Data Collection:** In addition to energy maximization, the proposed system also focuses on collecting real-time data on weather parameters such as temperature, humidity, and rainfall. These data can be used by farmers to make informed decisions regarding irrigation, pest control, and other crop management practices. The collected data are transferred to a mobile app, making it easier for farmers to access and utilize the information;
- **Hardware Experimental Setup:** A testbed with a hardware experimental setup is designed to evaluate the system's capability to track the sun effectively. This allows for practical testing and validation of the proposed approach;
- **Integration of AI Techniques:** The research incorporates AI techniques along with a QoS algorithm to improve the quality of service provided by the existing system. This integration enhances the overall performance and functionality of the system;

- **Improved Results:** The research demonstrates that the proposed system leads to a relative increase in efficiency of up to 52% compared to the existing system. These improved results highlight the effectiveness of the proposed approach in maximizing energy generation and providing valuable data for agricultural purposes.

In summary, the approach presented in this paper introduces a solar tracking system that enhances the efficiency of solar panels, collects real-time weather data, incorporates AI techniques, and achieves significant improvements in performance compared to the existing system.

3.6. Limitations and Future Work

The yearly energy efficiency results show that the values for dual-axis (98.7%), single-axis (98.2%), and fixed tilt (98.3%) are very close, and these small differences may not justify the added complexity and cost of dual-axis tracking. A fixed tilt system is likely much cheaper and simpler than a dual-axis tracker. The paper could have included estimated system costs and discussed whether the fractional efficiency gain of the dual-axis justifies the expense. A detailed cost–benefit analysis would strengthen these results in the future.

Similarly, highlighting the economic trade-offs and costs, not just the technical efficiency gains, would give a more complete picture, but this research focused on the technical capabilities of the dual-axis tracking system to optimize energy yield. Dual-axis tracking is a known technique, and the novelty lies in the application focus. The lack of economic analysis makes the real-world value unclear.

While this initial research focused primarily on demonstrating a proof of concept and evaluating the energy optimization capabilities, further studies on the reliability, robustness, and maintenance requirements would provide valuable additional insights. We could address reliability and maintainability in future work that includes the following:

- Conducting reliability engineering analyses such as FMEA to identify potential failure modes and their effects. This can help highlight vulnerabilities to be mitigated;
- Performing accelerated life testing on system components to evaluate lifespan and deterioration over time. These data can inform maintenance schedules;
- Implementing self-diagnostic features and fault-tolerant architectures to improve reliability and reduce downtime;
- Evaluating ease of repair, replacement, and upkeep to minimize maintenance labor time/costs;
- Considering the use of higher-durability components, weatherproofing, and corrosion-resistance to withstand harsh outdoor conditions;
- Analyzing tradeoffs between reliability gains and additional costs to find the optimal balance.

Incorporating these factors into future work on the solar tracking system could provide a more complete picture of overall performance and feasibility. While this research focused on the technical capabilities of the dual-axis tracking system to optimize energy yield, economic considerations are also important. As the paper notes in the introduction, a key challenge with solar PV is improving conversion efficiency and reducing manufacturing costs to be competitive with conventional power.

The work on comparing the costs of expanding the fixed array footprint versus adding dual-axis tracking is excellent. The paper compares energy efficiency metrics across different systems but does not factor in land usage. As the small footprint increase may be acceptable for agricultural applications, it is a good avenue for future work. Incorporating the economic analysis described would strengthen the paper by balancing the technical potential against practical cost factors in the future.

4. Conclusions

This research aimed to develop a dual-axis solar tracking system to enhance renewable energy optimization and collection from solar sources. The key goals were to improve solar panel efficiency, collect real-time weather data, and maximize energy yield through optimal panel orientation. The results demonstrated that the proposed approach increased efficiency by up to 52% compared to fixed solar panels. This aligned with the goal of optimizing efficiency through a tracking mechanism. The system also transmitted temperature, humidity, and air quality data to farmers via a mobile app. This achieved the objective of real-time data collection for agricultural applications. Additionally, the artificial neural network optimization increased performance stability, meeting the aim of incorporating AI techniques. The prototype testbed validated the ability to accurately track the sun's position, fulfilling the goal of experimental validation. Overall, the dual-axis control scheme optimized the solar panel orientation to maximize energy generation in alignment with the aims. The combination of efficiency gains, data collection capabilities, AI integration, and experimental validation demonstrate that the stated goals and objectives were achieved. While further work can build upon these results, this research makes significant contributions to developing an intelligent, high-efficiency solar tracking system with agricultural data monitoring. The outcomes provide a foundation for additional studies into reliability, economics, and end-user validation to strengthen real-world viability.

Author Contributions: Conceptualization, T.K., S.U.R. and T.A.; data curation, S.U.R. and T.A.; formal analysis, T.K.; funding acquisition, L.A.D.L.; investigation, K.M. and S.G.V.; methodology, T.A. and K.M.; resources, L.A.D.L.; software, S.G.V. and L.A.D.L.; supervision, I.A.; validation, I.A.; visualization, K.M. and S.G.V.; writing—original draft, T.K. and S.U.R.; writing—review & editing, I.A. All authors have read and agreed to the published version of the manuscript.

Funding: This research is funded by the European University of Atlantics.

Institutional Review Board Statement: Not applicable

Data Availability Statement: Not applicable.

Conflicts of Interest: The authors declare no conflict of interest.

References

1. Altwallbah, N.M.M.; Radzi, M.A.M.; Azis, N.; Shafie, S.; Zainuri, M.A.A.M. New perturb and observe algorithm based on trapezoidal rule: Uniform and partial shading conditions. *Energy Convers. Manag.* **2022**, *264*, 115738.
2. Abo-Khalil, A.G.; Alharbi, W.; Al-Qawasmi, A.R.; Alobaid, M.; Alarifi, I.M. Maximum power point tracking of PV systems under partial shading conditions based on opposition-based learning firefly algorithm. *Sustainability* **2021**, *13*, 2656.
3. Khalifa, A.E.; Refaat, A.; Kalas, A.; Elfar, M.H. Two Bio-inspired MPPT Algorithms to Harvest the Maximum Power from Partially Shaded PV Arrays. In Proceedings of the 2022 Conference of Russian Young Researchers in Electrical and Electronic Engineering (ElConRus), St. Petersburg, Russia, 25–28 January 2022; pp. 670–674.
4. Refaat, A.; Osman, M.H.; Korovkin, N.V. Current collector optimizer topology to extract maximum power from non-uniform aged PV array. *Energy* **2020**, *195*, 116995.
5. Elsakka, M.M.; Ingham, D.B.; Ma, L.; Pourkashanian, M. Comparison of the computational fluid dynamics predictions of vertical axis wind turbine performance against detailed pressure measurements. *Int. J. Renew. Energy Res.* **2021**, *11*, 276–293.
6. Abuhashish, M.N.; Daoud, A.A.; Elfar, M.H. A Novel Model Predictive Speed Controller for PMSG in Wind Energy Systems. *Int. J. Renew. Energy Res.* **2022**, *12*, 170–180.
7. Amer, A.E.; Elsakka, M.M.; Lebedev, V.A. Thermal performance of an accumulator unit using phase change material with a fixed volume of fins. *Int. J. Energy Res.* **2021**, *45*, 19089–19102.
8. Boriskina, S.V.; Tong, J.K.; Hsu, W.C.; Weinstein, L.; Huang, X.; Loomis, J.; Xu, Y.; Chen, G. Hybrid optical-thermal devices and materials for light manipulation and radiative cooling. In Proceedings of the Active Photonic Materials VII, San Diego, CA, USA, 9–13 August 2015; Volume 9546, pp. 190–196.
9. Joisher, M.; Singh, D.; Taheri, S.; Espinoza-Trejo, D.R.; Pouresmaeil, E.; Taheri, H. A hybrid evolutionary-based MPPT for photovoltaic systems under partial shading conditions. *IEEE Access* **2020**, *8*, 38481–38492.
10. Ram, J.P.; Rajasekar, N. A new global maximum power point tracking technique for solar photovoltaic (PV) system under partial shading conditions (PSC). *Energy* **2017**, *118*, 512–525.
11. Refaat, A.; Osman, M. Current collector optimizer topology to improve maximum power from PV array under partial shading conditions. *IOP Conf. Ser. Mater. Sci. Eng.* **2019**, *643*, 012094.

12. Hassan, A.; Bass, O.; Masoum, M.A. An improved genetic algorithm based fractional open circuit voltage MPPT for solar PV systems. *Energy Rep.* **2023**, *9*, 1535–1548.
13. Verma, P.; Garg, R.; Mahajan, P. Asymmetrical interval type-2 fuzzy logic control based MPPT tuning for PV system under partial shading condition. *ISA Trans.* **2020**, *100*, 251–263.
14. Refaat, A.; Elgamal, M.; Korovkin, N.V. A novel photovoltaic current collector optimizer to extract maximum power during partial shading or mismatch conditions. In Proceedings of the 2019 IEEE Conference of Russian Young Researchers in Electrical and Electronic Engineering (EIConRus), St. Petersburg/Moscow, Russia, 28–31 January 2019; pp. 407–412.
15. Osman, M.H.; Ahmed, M.K.; Refaat, A.; Korovkin, N.V. A comparative study of MPPT for PV system based on modified perturbation & observation method. In Proceedings of the 2021 IEEE Conference of Russian Young Researchers in Electrical and Electronic Engineering (ElConRus), St. Petersburg/Moscow, Russia, 26–29 January 2021; pp. 1023–1026.
16. Osman, M.H.; Elseify, M.A.; Ahmed, M.K.; Korovkin, N.V.; Refaat, A. Highly Efficient MPP Tracker based on Adaptive Neuro-fuzzy Inference System for Stand-Alone Photovoltaic Generator System. *Int. J. Renew. Energy Res.* **2022**, *12*, 208–217.
17. Narasimman, K.; Gopalan, V.; Bakthavatsalam, A.; Elumalai, P.; Shajahan, M.I.; Michael, J.J. Modelling and real time performance evaluation of a 5 MW grid-connected solar photovoltaic plant using different artificial neural networks. *Energy Convers. Manag.* **2023**, *279*, 116767.
18. Azli, H.; Titri, S.; Larbes, C.; Kaced, K.; Femmam, K. Novel yellow saddle goatfish algorithm for improving performance and efficiency of PV system under partial shading conditions. *Sol. Energy* **2022**, *247*, 295–307.
19. Ahmed, J.; Salam, Z. A Maximum Power Point Tracking (MPPT) for PV system using Cuckoo Search with partial shading capability. *Appl. Energy* **2014**, *119*, 118–130.
20. Mirza, A.F.; Ling, Q.; Javed, M.Y.; Mansoor, M. Novel MPPT techniques for photovoltaic systems under uniform irradiance and Partial shading. *Sol. Energy* **2019**, *184*, 628–648.
21. Aouchiche, N.; Aitcheikh, M.; Becherif, M.; Ebrahim, M.A. AI-based global MPPT for partial shaded grid connected PV plant via MFO approach. *Sol. Energy* **2018**, *171*, 593–603.
22. Mohanty, S.; Subudhi, B.; Ray, P.K. A new MPPT design using grey wolf optimization technique for photovoltaic system under partial shading conditions. *IEEE Trans. Sustain. Energy* **2015**, *7*, 181–188.
23. Liu, H.D.; Lin, C.H.; Pai, K.J.; Wang, C.M. A GMPPT algorithm for preventing the LMPP problems based on trend line transformation technique. *Sol. Energy* **2020**, *198*, 53–67.
24. Mansoor, M.; Mirza, A.F.; Ling, Q. Harris hawk optimization-based MPPT control for PV systems under partial shading conditions. *J. Clean. Prod.* **2020**, *274*, 122857.
25. Mirza, A.F.; Mansoor, M.; Ling, Q. A novel MPPT technique based on Henry gas solubility optimization. *Energy Convers. Manag.* **2020**, *225*, 113409.
26. Chandrasekaran, K.; Sankar, S.; Banumalar, K. Partial shading detection for PV arrays in a maximum power tracking system using the sine-cosine algorithm. *Energy Sustain. Dev.* **2020**, *55*, 105–121.
27. Fares, D.; Fathi, M.; Shams, I.; Mekhilef, S. A novel global MPPT technique based on squirrel search algorithm for PV module under partial shading conditions. *Energy Convers. Manag.* **2021**, *230*, 113773.
28. Eltamaly, A.M.; Al-Saud, M.; Abokhalil, A.G.; Farh, H.M. Simulation and experimental validation of fast adaptive particle swarm optimization strategy for photovoltaic global peak tracker under dynamic partial shading. *Renew. Sustain. Energy Rev.* **2020**, *124*, 109719.
29. Mirza, A.F.; Mansoor, M.; Ling, Q.; Yin, B.; Javed, M.Y. A Salp-Swarm Optimization based MPPT technique for harvesting maximum energy from PV systems under partial shading conditions. *Energy Convers. Manag.* **2020**, *209*, 112625.
30. Lyden, S.; Haque, M.E. A simulated annealing global maximum power point tracking approach for PV modules under partial shading conditions. *IEEE Trans. Power Electron.* **2015**, *31*, 4171–4181.
31. Mansoor, M.; Mirza, A.F.; Ling, Q.; Javed, M.Y. Novel Grass Hopper optimization based MPPT of PV systems for complex partial shading conditions. *Sol. Energy* **2020**, *198*, 499–518.
32. Eltamaly, A.M. An improved cuckoo search algorithm for maximum power point tracking of photovoltaic systems under partial shading conditions. *Energies* **2021**, *14*, 953.
33. Guo, K.; Cui, L.; Mao, M.; Zhou, L.; Zhang, Q. An improved gray wolf optimizer MPPT algorithm for PV system with BFBIC converter under partial shading. *IEEE Access* **2020**, *8*, 103476–103490.
34. Motamarri, R.; Bhookya, N.; Chitti Babu, B. Modified grey wolf optimization for global maximum power point tracking under partial shading conditions in photovoltaic system. *Int. J. Circuit Theory Appl.* **2021**, *49*, 1884–1901.
35. Obukhov, S.; Ibrahim, A.; Diab, A.A.Z.; Al-Sumaiti, A.S.; Aboelsaud, R. Optimal performance of dynamic particle swarm optimization based maximum power trackers for stand-alone PV system under partial shading conditions. *IEEE Access* **2020**, *8*, 20770–20785.
36. Mirza, A.F.; Mansoor, M.; Zhan, K.; Ling, Q. High-efficiency swarm intelligent maximum power point tracking control techniques for varying temperature and irradiance. *Energy* **2021**, *228*, 120602.

37. Chai, L.G.K.; Gopal, L.; Juwono, F.H.; Chiong, C.W.; Ling, H.C.; Basuki, T.A. A novel global MPPT technique using improved PS-FW algorithm for PV system under partial shading conditions. *Energy Convers. Manag.* **2021**, *246*, 114639.
38. Gong, L.; Hou, G.; Huang, C. A two-stage MPPT controller for PV system based on the improved artificial bee colony and simultaneous heat transfer search algorithm. *ISA Trans.* **2023**, *132*, 428–443.